

## Article (refereed) - postprint

---

Oulehle, Filip; Kopáček, Jiří; Chuman, Tomáš; Černohous, Vladimír; Hůnová, Iva; Hruška, Jakub; Krám, Pavel; Lachmanová, Zora; Navrátil, Tomáš; Štěpánek, Petr; Tesař, Miroslav; Evans, Christopher D. 2016.  
**Predicting sulphur and nitrogen deposition using a simple statistical method.**

© 2016 Elsevier Ltd.

This manuscript version is made available under the CC-BY-NC-ND 4.0 license <http://creativecommons.org/licenses/by-nc-nd/4.0/>



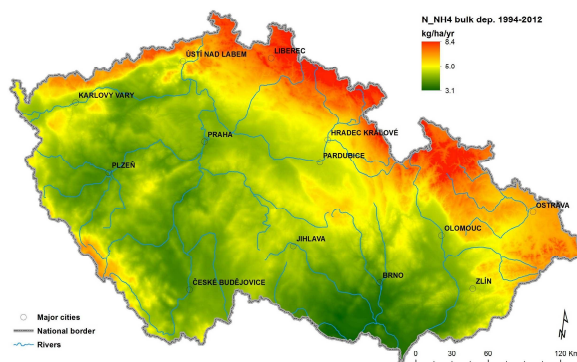
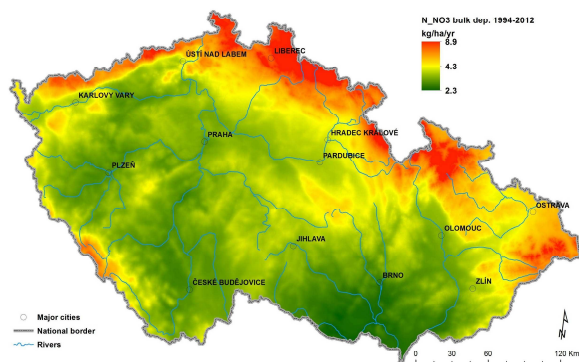
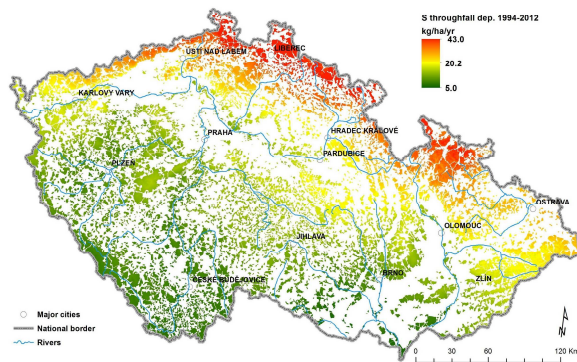
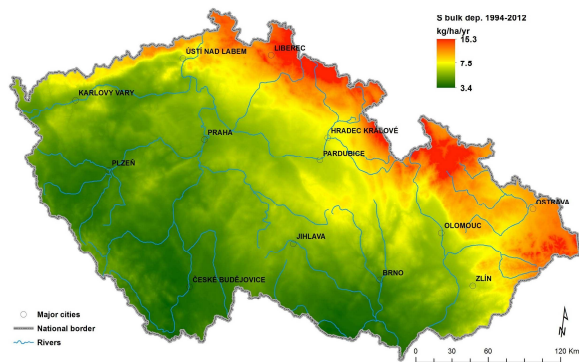
This version available <http://nora.nerc.ac.uk/515665/>

NERC has developed NORA to enable users to access research outputs wholly or partially funded by NERC. Copyright and other rights for material on this site are retained by the rights owners. Users should read the terms and conditions of use of this material at <http://nora.nerc.ac.uk/policies.html#access>

NOTICE: this is the author's version of a work that was accepted for publication in *Atmospheric Environment*. Changes resulting from the publishing process, such as peer review, editing, corrections, structural formatting, and other quality control mechanisms may not be reflected in this document. Changes may have been made to this work since it was submitted for publication. A definitive version was subsequently published in *Atmospheric Environment* (2016), 140. 456-468. [10.1016/j.atmosenv.2016.06.028](https://doi.org/10.1016/j.atmosenv.2016.06.028)

[www.elsevier.com/](http://www.elsevier.com/)

Contact CEH NORA team at  
[noraceh@ceh.ac.uk](mailto:noraceh@ceh.ac.uk)



ACCEPTED MANUSCRIPT

# Predicting sulphur and nitrogen deposition using a simple statistical method

Oulehle Filip<sup>a\*</sup>, Kopáček Jiří<sup>b,c</sup>, Chuman Tomáš<sup>a</sup>, Černohous Vladimír<sup>d</sup>, Hůnová Iva<sup>e</sup>, Hruška Jakub<sup>a</sup>, Krám Pavel<sup>f</sup>, Lachmanová Zora<sup>d</sup>, Navrátil Tomáš<sup>g</sup>, Štěpánek Petr<sup>f</sup>, Tesař Miroslav<sup>h</sup>, Evans D. Christopher<sup>i</sup>

<sup>a</sup> Czech Geological Survey, Klárov 3, 118 21 Prague, Czech Republic

<sup>b</sup> Biology Centre CAS, Institute of Hydrobiology, Na Sádkach 7, 370 05 České Budějovice, Czech Republic

<sup>c</sup> University of South Bohemia, Faculty of Science, České Budějovice, Czech Republic

<sup>d</sup> Forestry and Game Management Research Institute, Strnady 136, 252 02 Jíloviště, Czech Republic

<sup>e</sup> Czech Hydrometeorological Institute, Na Šabatce 2050/17, 143 06 Prague, Czech Republic

<sup>f</sup> Global Change Research Institute, AS CR, Bělidla 986/4a, 603 00 Brno, Czech Republic

<sup>g</sup> Institute of Geology, AS CR, Rozvojevá 269, 165 00 Prague, Czech Republic<sup>g</sup>

<sup>h</sup> Institute of Hydrodynamics, AS CR, Pod Patankou 30/5, 160 00 Prague, Czech Republic

<sup>i</sup> Centre for Ecology and Hydrology, Bangor LL57 2UW, UK

\*Corresponding author. E-mail address: [filip.oulehle@geology.cz](mailto:filip.oulehle@geology.cz)

## HIGHLIGHTS

- Temporal coherence of precipitation SO<sub>4</sub>, NO<sub>3</sub> and NH<sub>4</sub> was demonstrated
- Regional S and N emissions enabled to reconstruct long-term changes in deposition
- Empirically-based interpolation allowed spatial deposition variations to be mapped

## ABSTRACT

Data from 32 long-term (1994 – 2012) monitoring sites were used to assess temporal development and spatial variability of sulphur (S) and inorganic nitrogen (N) concentrations in bulk precipitation, and S in throughfall, for the Czech Republic. Despite large variance in absolute S and N concentration/deposition among sites, temporal coherence using standardized data (Z score) was demonstrated. Overall significant declines of SO<sub>4</sub> concentration in bulk and throughfall precipitation, as well as NO<sub>3</sub> and NH<sub>4</sub> concentration in bulk precipitation, were observed. Median Z score values of bulk SO<sub>4</sub>, NO<sub>3</sub> and NH<sub>4</sub> and throughfall SO<sub>4</sub> derived from observations and the respective emission rates of SO<sub>2</sub>, NO<sub>x</sub> and NH<sub>3</sub> in the Czech Republic and Slovakia showed highly significant ( $p < 0.001$ ) relationships. Using linear regression models, Z score values were calculated for the whole period 1900 - 2012 and then back-transformed to give estimates of concentration for the individual sites. Uncertainty associated with the concentration calculations was estimated as 20 % for SO<sub>4</sub> bulk precipitation, 22 % for throughfall SO<sub>4</sub>, 18 % for bulk NO<sub>3</sub> and 28 % for bulk NH<sub>4</sub>. The application of the method suggested that it is effective in the long-term reconstruction and prediction of S and N deposition at a variety of sites. Multiple regression modelling was used to extrapolate site characteristics (mean precipitation chemistry and its standard deviation) from monitored to unmonitored sites. Spatially distributed temporal development of S and N depositions were calculated since 1900. The method allows spatio-temporal estimation of the acid deposition in regions with extensive monitoring of precipitation chemistry.

**Keywords:** precipitation, sulphur, nitrogen, deposition, monitoring, upscaling

49 **1 INTRODUCTION**

50  
51 The acidification of sensitive ecosystems by sulphur (S) and nitrogen (N) deposition has been a  
52 widespread environmental problem in Europe since the mid 20<sup>th</sup> century. More recently, there has  
53 been increasing concern that elevated atmospheric N inputs are leading to eutrophication of semi-  
54 natural ecosystems (Bobbink et al., 2010). Monitoring data for the main driving variables, the  
55 deposition of S and N species, are generally available only for a relatively short period (Schöpp et al.,  
56 2003). Therefore estimations of S and N deposition levels over longer periods are based on emission  
57 trends (Kopacek et al., 2001; Schöpp et al., 2003). Knowledge of the emission history and deposition  
58 trends of major acidifying pollutants is a key factor for understanding changes in those ecosystems,  
59 and in particular is an important input to process-based models used to predict the long-term  
60 impacts of atmospheric deposition on terrestrial and aquatic ecosystems (Bonten et al., 2016;  
61 Hofmeister et al., 2008; Oulehle et al., 2015).

62 On a European scale, the EMEP (European Monitoring and Evaluation Programme) Eulerian acid  
63 deposition model (Simpson et al., 2003) is used to simulate sulphur, nitrogen oxides and ammonia  
64 deposition in grid cells at a 50 km × 50 km resolution. This model has provided the basis for  
65 optimisation of emissions control legislation at a European scale within the UNECE Convention on  
66 Long-Range Transboundary Air Pollution (CLRTAP), most recently the Gothenburg Protocol (UNECE,  
67 2004). However, the low spatial resolution of this model may lead to a high within-grid cell  
68 variability, particularly in topographically complex areas, and also provides average rather than  
69 ecosystem-specific (e.g. forest versus grassland) deposition. As a result, it is difficult to relate the  
70 large-scale model simulations to specific sites or ecosystems.

71 According to the Gothenburg Protocol, the respective SO<sub>2</sub>, NO<sub>x</sub> and NH<sub>3</sub> emissions should have been  
72 85%, 61% and 35% lower in the Czech Republic in 2010 compared to the 1990 base line. However,  
73 already by 2007, SO<sub>2</sub> emissions had decreased by 88% to 217 kt yr<sup>-1</sup>, NO<sub>x</sub> emissions by 62% to 284 kt  
74 yr<sup>-1</sup> and NH<sub>3</sub> emissions by 62% to 60 kt yr<sup>-1</sup> ([www.emep.int](http://www.emep.int)), therefore target emissions have been  
75 successfully passed. The decrease of SO<sub>2</sub> emissions in the Czech Republic has been one of the most  
76 pronounced examples of pollution reduction anywhere in Europe (Vestreng et al., 2007), and are  
77 believed to have had profound consequences for ecosystem biogeochemistry including the carbon  
78 and nitrogen cycles (Oulehle et al., 2011).

79 Many countries provide long-term air quality monitoring including assessment of spatial and  
80 temporal changes in precipitation chemistry (wet-only, bulk, throughfall), such as National  
81 atmospheric deposition program (NADP) across USA and European Monitoring and Evaluation  
82 Programme (EMEP) under CLRTAP. European nation based programs operate across many countries  
83 (e.g. SWETHRO in Sweden, UKEAP in the UK or GEOMON in the Czech Republic). Precipitation  
84 composition often integrates altered air quality over large parts of landscape, thus common  
85 coherence in chemistry trends across different monitoring sites may be expected and explored.  
86 However, air quality is influenced by different sources of emissions, thus S deposition might be  
87 influenced directly by SO<sub>2</sub> emissions cuts from big stationary sources over large areas, whereas N  
88 deposition may behave less consistently due to the mixing of emissions from small (local) and large  
89 stationary sources, as well as mobile (transport) sources (Waldner et al., 2014). Geographical  
90 features (e.g. local topography) may also determine different levels and temporal pattern of S and N  
91 deposition at sites in the same area (Rogora et al., 2006). Here, we use all stations with available data  
92 on precipitation chemistry in the Czech Republic spanning at least 15 years to examine the  
93 spatiotemporal variations in SO<sub>4</sub>, NH<sub>4</sub> and NO<sub>3</sub> concentrations and fluxes in bulk precipitation and  
94 throughfall (only SO<sub>4</sub>) in this central European region. Specifically, we (i) evaluate the degree of  
95 underlying coherence in deposition trends across the range of monitoring sites, (ii) develop and test  
96 a methodology enabling to infer S and N deposition across the spatio-temporal gradients in a study  
97 region from the related emission trends, and (iii) apply this method to reconstruct historical trends in  
98 S and N deposition in the Czech Republic back to 1900.

99

## 100 2 MATERIALS AND METHODS

101

### 102 2.1 STATION DATA DESCRIPTION

103

104 The monitoring stations of precipitation chemistry are located in the Czech Republic and close border  
105 areas (Slovakia and Austria) and comprise 32 stations. For their location see the Supplementary  
106 Information (SI; Figure S1). Site elevations varied between 180 (Praha-Podbaba) and 2023 m a. s. l.  
107 (Chopok station, Slovakia) and mean annual precipitation depths varied between 503 and 1641 mm  
108  $\text{yr}^{-1}$  during 1961 – 2012. The number of years with available volume weighted mean chemistry varied  
109 from 15 to 35 years for individual stations and cover the period from 1978 to 2012 (Table S1).  
110 Monitoring stations differ in frequency of precipitation sampling and type of precipitation samplers.  
111 The rain water collection comprises daily, weekly and monthly sampling, dependent on site manager.  
112 We used only annual weighted means. Precipitation collectors comprise open bulk collectors and wet  
113 only collectors. Fifteen stations provide throughfall (under the Norway spruce - the dominant tree in  
114 the Czech forests) precipitation chemistry data.

115 We used sulphate ( $\text{SO}_4$ ), nitrate ( $\text{NO}_3$ ) and ammonium ( $\text{NH}_4$ ) concentrations. In general,  $\text{SO}_4$  and  $\text{NO}_3$   
116 were measured by ion chromatography,  $\text{NH}_4$  either by potentiometry or by manual/automatic  
117 spectrophotometric determination by the indophenol blue method (analytical procedures have  
118 changed since 1976, thus for further details visit:  
119 [http://www.chmi.cz/files/portal/docs/uoco/web\\_generator/locality/precipitation\\_locality/index\\_GB.](http://www.chmi.cz/files/portal/docs/uoco/web_generator/locality/precipitation_locality/index_GB.html)  
120 [html](http://www.chmi.cz/files/portal/docs/uoco/web_generator/locality/precipitation_locality/index_GB.html)). The reliability of the chemical data was controlled by means of an ionic balance for the annual  
121 average concentrations. Data with differences between the sum of cations and the sum of anions  
122 lower than  $\pm 10\%$  of the total ionic content were used without any other control. If the difference  
123 exceeded  $\pm 10\%$ , the data were checked for errors using a trend analysis. If the concentration of  
124 some ion was outlying the trend and at the same time this difference from the trend explained the  
125 error in the ionic balance control, we excluded this ion from other analyses, but used the rest of the  
126 data on chemical composition.

127

### 128 2.2 $\text{SO}_2$ , $\text{NO}_x$ AND $\text{NH}_3$ EMISSIONS

129

130 Historical Czech and Slovak (CS) emission trends for  $\text{SO}_2$ ,  $\text{NO}_x$ , and  $\text{NH}_3$  are based on data from the  
131 official databases of EMEP ([www.ceip.at/emission-data-webdab](http://www.ceip.at/emission-data-webdab)) for the 1980 – 2012 period, and on  
132 data calculated by (Kopacek and Vesely, 2005) for the 1900 – 1990 period. The calculated CS  
133 emissions of anthropogenic  $\text{SO}_2$ ,  $\text{NO}_x$ , and  $\text{NH}_3$  were on average 7 % higher, 2 % lower, and 8 %  
134 higher, respectively, than the EMEP data for the overlapping 1980 – 1990 period. Data on central  
135 European (Austria + Germany + Poland + CS) emissions of  $\text{SO}_2$  and  $\text{NO}_x$  and  $\text{NH}_3$  after 1980 were  
136 taken from the EMEP database; emissions of  $\text{SO}_2$  and  $\text{NO}_x$  before 1980 are from Mylona (1996) and  
137 Schöpp et al. (2003), respectively. Data on central European emissions of  $\text{NH}_3$  prior to 1980 were  
138 calculated for individual countries using inventories of livestock, use of synthetic N-fertilizers (FAO  
139 database, <http://faostat.fao.org>), and data on population, using the per-capita emission model  
140 (Kopáček and Posch, 2011).

141 The long-term trend in CS emissions of  $\text{SO}_2$  was similar to the central European trend, except for  
142 1970 - 1990, when CS emissions increased more sharply due to high emission rates in the region  
143 (Figure 1). The CS emission rate of  $\text{NH}_3$  was lower than that in the central Europe and decreased  
144 more in the 1990s, due predominantly to lower areal livestock density and its larger reduction in CS  
145 than in Germany. Central European emissions of  $\text{NO}_x$  were slightly lower in the 1980s and trends  
146 were similar to the CS trend in 1990s.

147

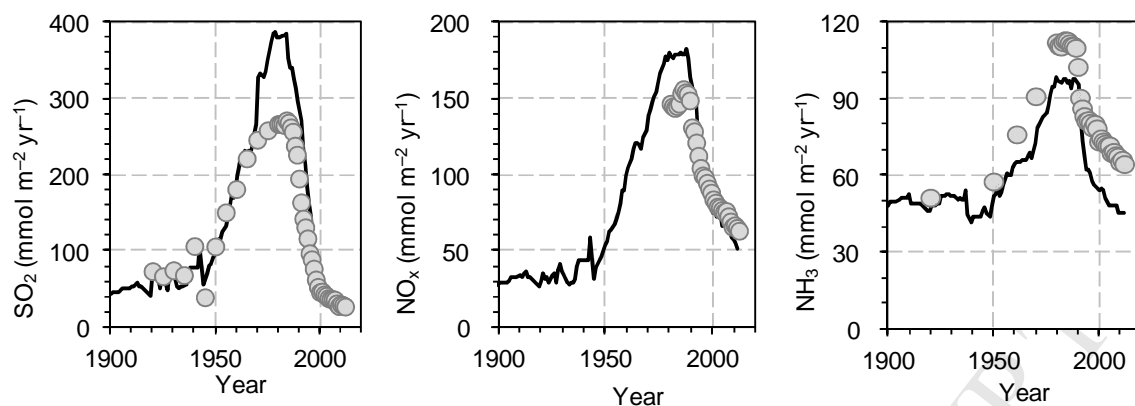


Figure 1. Historical trends (1900 - 2012) in emissions of  $\text{SO}_2$ ,  $\text{NO}_x$  and  $\text{NH}_3$  in the area of the Czech and Slovak Republic (CS, black line) and in central Europe (circles; Austria, Germany, Poland and CS).

## 2.3 TIME SERIES STANDARDISATION

### 2.3.1 Precipitation chemistry data processing

Recalculation of wet only  $\text{SO}_4$ ,  $\text{NO}_3$  and  $\text{NH}_4$  concentrations to bulk precipitation was based on parallel measurements of wet - only and bulk precipitation on eleven stations. For  $\text{SO}_4$ , 64 parallel annual measurements (Figure 2) were available and a linear regression model was obtained:

$$\text{SO}_4 \text{ bulk } (\mu\text{eq L}^{-1}) = 1.04 \times \text{SO}_4 \text{ wet } (\mu\text{eq L}^{-1}) + 21.99 \quad (1)$$

For  $\text{NO}_3$ , 51 parallel annual measurements (Figure 2) were obtained and the linear regression model was:

$$\text{NO}_3 \text{ bulk } (\mu\text{eq L}^{-1}) = 0.87 \times \text{NO}_3 \text{ wet } (\mu\text{eq L}^{-1}) + 14.87 \quad (2)$$

For  $\text{NH}_4$ , 45 parallel annual measurements (Figure 2) were obtained and the linear regression model was:

$$\text{NH}_4 \text{ bulk } (\mu\text{eq L}^{-1}) = 1.01 \times \text{NH}_4 \text{ wet } (\mu\text{eq L}^{-1}) + 18.93 \quad (3)$$

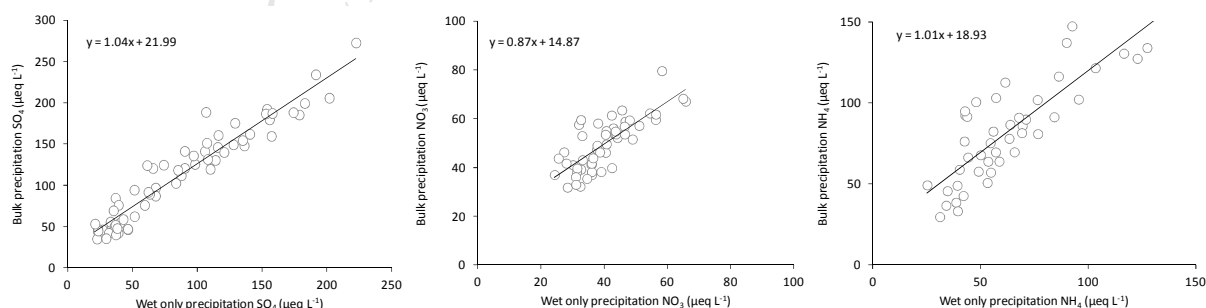


Figure 2. Relationships between available annual volume weighted mean concentrations of  $\text{SO}_4$ ,  $\text{NO}_3$  and  $\text{NH}_4$  in wet-only and bulk precipitation in the Czech Republic.

### 2.3.2 Site standardization

181 Despite large variance in precipitation chemistry across sites, underlying patterns of temporal  
 182 variation show strong similarities. To demonstrate these underlying patterns, measured annual  
 183 concentration of  $\text{SO}_4$ ,  $\text{NH}_4$  and  $\text{NO}_3$  at each sampling site  $s$  on respective year  $t$  ( $C_{st}$ ) were  
 184 standardised over time, by subtracting the site mean ( $C_s$ ) for the whole time series (1994–2012) and  
 185 dividing by the site standard deviation ( $\sigma_s$ ) according to:

$$187 \quad Z_{st} = \frac{C_{st} - C_s}{\sigma_s} \quad (4)$$

188  
 189 The time series of standardised concentrations ( $Z_{st}$  referred to as ‘Z score’) thus have a zero mean  
 190 and a standard deviation equal to 1. This implies that temporal effects are essentially multiplicative,  
 191 so that sites with generally high concentrations will tend to have high variability over time in absolute  
 192 but not in relative terms (Evans et al., 2010). The degree of observed between - site coherence was  
 193 quantified as the mean annual 10<sup>th</sup> - 90<sup>th</sup> percentile Z score range for all sites over the monitoring  
 194 period, following the method of Evans et al. (2010).

### 196 2.3.3 Historical trends estimations

197  
 198 Median Z scores for  $\text{SO}_4$ ,  $\text{NH}_4$  and  $\text{NO}_3$  in bulk precipitation and for  $\text{SO}_4$  in throughfall for each year  
 199 across the whole set of sites was calculated according to Eq. 4. Obtained median values were then  
 200 related to emissions by linear regression method for the period 1994 - 2012. We used logarithmically  
 201 transformed emission data because they were better fitted by the regression model than non-  
 202 transformed data. For the modelling we used the CS emission trends because they provided closer  
 203 relationships with the deposition data than the central European trends. The obtained equations  
 204 were then used to calculate median  $\text{SO}_4$ ,  $\text{NH}_4$  and  $\text{NO}_3$  Z scores for their concentrations in the whole  
 205 1900 - 2012 period according to the respective emission rates of  $\text{SO}_2$ ,  $\text{NH}_3$  and  $\text{NO}_x$  (Figure 1).  
 206 The median time series of Z scores for whole set of sites was then back-transformed to give  
 207 estimates of  $C_{st}$  for each individual site for the whole period 1900–2012 according to Eq. 5, and  
 208 following the notation of Eq. 4:

$$209 \quad C_{st} = (Z_{st} \times \sigma_s) + C_s \quad (5)$$

210 The  $C_s$  and the  $\sigma_s$  were calculated from the measured data between 1994 and 2012.

### 215 2.3.4 Model validation

216  
 217 Results obtained for individual sites according to Eq. 5 were compared with measured  
 218 concentrations. The precision of the model outputs was calculated by three measures; the Root  
 219 Mean Square Error (RMSE), Nash-Sutcliffe Coefficient of Determination (NSCD) and a linear  
 220 regression coefficient ( $R^2$ ) were used to assess explained variability of model estimations (De Vries et  
 221 al., 2010; Janssen and Heuberger, 1995; Nash and Sutcliffe, 1970).

$$222 \quad RMSE = \sqrt{\frac{\sum_{i=1}^N (P_i - O_i)^2}{N}} \quad (6)$$

$$223 \quad NSCD = \sqrt{\frac{\sum_{i=1}^N (O_i - P_i)^2}{\sum_{i=1}^N (O_i - O)^2}} \quad (7)$$

224  
 225  
 226  
 227 Where  $P_i$  is predicted value,  $O_i$  is observed value,  $O$  is average of observed values and  $N$  is number of  
 228 observations.

229 RMSE describes the deviations between the measurements and the predictions in a quadratic way  
230 and is thus rather sensitive to extreme values. RMSE has the same units as the quantity being  
231 estimated. An NSCD of 0 indicates that the model predictions are as accurate as the mean of the  
232 observed data; the closer the model is to 1, the more accurate the model is.

233 Finally, we used long-term precipitation chemistry (with years of observations before 1994) from  
234 bulk precipitation ANE, JEZ, LYS, NAC, SLA and PCJ (for site abbreviations see SI, Table S1) sites to  
235 compare model outputs with measured chemistry within the period 1978 - 2012. This comparison  
236 highlighted the model performance at the time of the highest measured S and N depositions across  
237 Central Europe.

238

## 239 **2.4 SPATIAL PRECIPITATION CHEMISTRY MODEL**

240

241 The large number of sites with measured precipitation chemistry across the study region allowed us  
242 to test whether site characteristics (coordinates, elevation, precipitation amount) may be used to  
243 calculate site  $C_s$  and  $\sigma_s$ , and thus to estimate site precipitation chemistry at any given position and  
244 year within the period 1900 and 2012, according to Eq. 5.

245 We used multiple regression analysis to study the relationship between dependent (response)  
246 variables and independent variables (predictors) derived from 32 stations. Selection of predictors  
247 was based on stepwise regression with forward selection method. The forward selection method, at  
248 each step, selects the candidate variable that increases  $R^2$  the most. It stops when none of the  
249 remaining variables are significant. Outliers can have a large impact on this stepping procedure, so  
250 we made some attempt to remove outliers from dataset before applying this method.

251 Independent variables entering the stepwise regression model were: latitude ( $X$ ), longitude ( $Y$ ),  
252 precipitation depth ( $P$ ; mm) and elevation ( $E$ ; m a.s.l.). Latitude and longitude are expressed in  
253 Křovák's projection (JTSK).

254

### 255 **2.4.1 Model validation**

256

257 Results obtained for individual sites ( $C_{S_{SO_4}}$ ,  $C_{S_{SO_4}thf}$ ,  $C_{S_{NO_3}}$ ,  $C_{S_{NH_4}}$ ,  $\Delta C_{S_{SO_4}}$ ,  $\Delta C_{S_{SO_4}thf}$ ,  $\Delta C_{S_{NO_3}}$ ,  $\Delta C_{S_{NH_4}}$ ,  $\sigma_{S_{SO_4}}$ ,  
258  $\sigma_{S_{SO_4}thf}$ ,  $\sigma_{S_{NO_3}}$ ,  $\sigma_{S_{NH_4}}$ ), where  $\Delta C_s$  represents annual rate of solute change in  $\mu\text{eq L}^{-1} \text{year}^{-1}$ , were  
259 compared with measured concentrations. The precision of the model outputs was calculated by  
260 Nash-Sutcliffe coefficient of determination (NSCD) and RMSE was used to assess explained variability  
261 of model estimations (Janssen and Heuberger, 1995; de Vries et al., 2010; Nash and Sutcliffe, 1970).

### 262 **2.4.2 Average precipitation estimates and deposition calculations**

263

264 Precipitation data were estimated from a dataset of about 200 stations (obtained from Czech  
265 Hydrometeorological Institute) distributed around the Czech Republic. After the quality control and  
266 homogenization (methods are described e.g. in Štěpánek et al., (2013)) new series for given  
267 individual sites were calculated. The calculation of the "new" series was based on geostatistical  
268 interpolation methods, improved by standardization of neighbouring stations values to altitude of a  
269 given location by means of regional regression analysis (Štěpánek et al., 2011). Parameters settings of  
270 the calculation differ for each meteorological element and optimal settings were found by means of  
271 cross validation. In this case, series for a given site were obtained from up to 6 nearest stations  
272 within maximum distance of 50 km, with the allowed maximum difference in altitude of 700 m.  
273 Before applying inverse distance weighting, data at the adjacent stations were standardized relative  
274 to the altitude of the base grid point (station location). The standardization was carried out by means  
275 of linear regression, dependence of values of a particular meteorological element on altitude, for  
276 each day individually, and regionally. Each standardized value was checked to ensure that it did not  
277 differ excessively from the original value. Modelled precipitation was used to calculate deposition of



278 S and N based on estimated  $\text{SO}_4$ ,  $\text{NO}_3$  and  $\text{NH}_4$  concentrations in precipitation. Median calculated  
279 bulk deposition for the Czech Republic was based on 1599 points regularly distributed across the  
280 Czech Republic, thus each point represented an area of  $49 \text{ km}^2$ . Median calculated throughfall S  
281 deposition for the Czech Republic was based on 499 points, representing forested areas.

282

## 283 **3 RESULTS AND DISCUSSION**

---

284

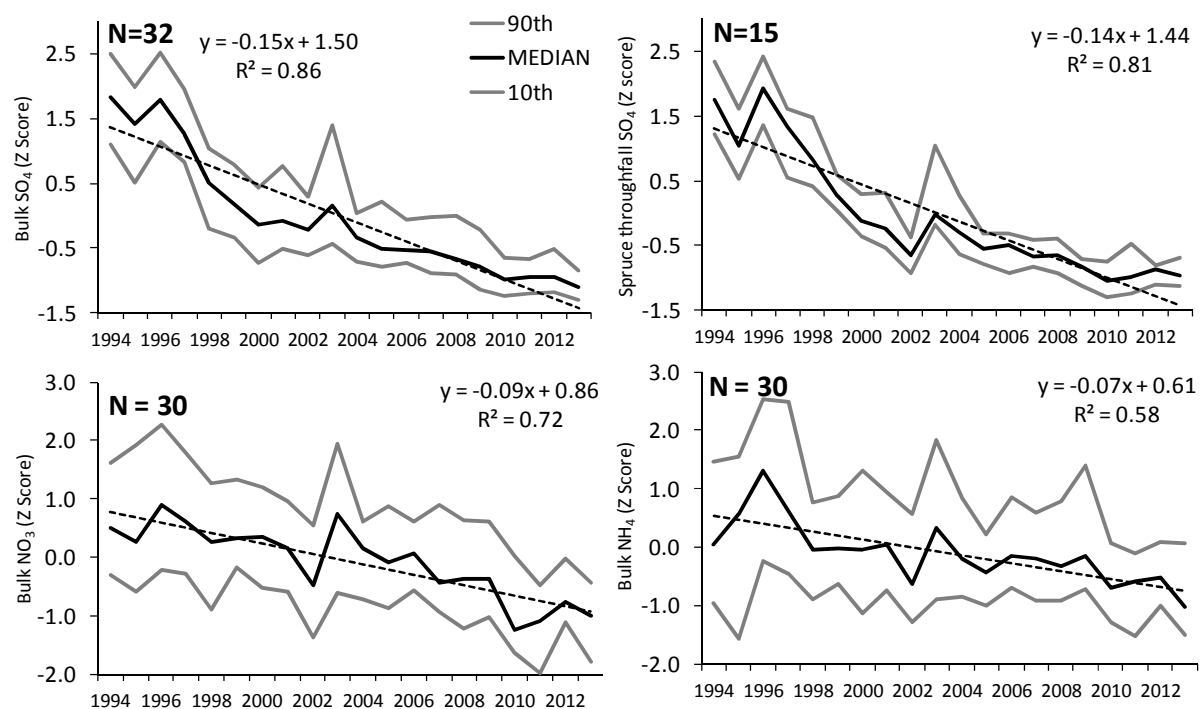
### 285 **3.1 MEASURED TRENDS OF $\text{SO}_4$ , $\text{NH}_4$ AND $\text{NO}_3$ CONCENTRATIONS**

286

287 Annual mean  $\text{SO}_4$ ,  $\text{NH}_4$  and  $\text{NO}_3$  concentrations in precipitation differed significantly across individual  
288 sites (Table S1). Despite high between-site variability of mean concentrations, standardization  
289 highlights the degree of underlying temporal coherence in the measured dataset (Figure 3). A highly  
290 significant decline in  $\text{SO}_4$  annual average precipitation concentration ( $R^2 = 0.86$  versus year,  $p <$   
291  $0.001$ ), as well as throughfall concentration ( $R^2 = 0.81$  versus year,  $p < 0.001$ ), was observed during  
292 the 1990s and 2000s. Moreover, both bulk precipitation and throughfall  $\text{SO}_4$  concentrations showed  
293 high inter-site coherence (mean annual 10<sup>th</sup> - 90<sup>th</sup> percentile range of 1.04 and 0.74 standardised  
294 units, respectively). For  $\text{NO}_3$  concentrations in bulk precipitation, a significant decline was observed  
295 in median trend ( $R^2 = 0.72$  versus time,  $p < 0.001$ ), with higher inter-site variability (mean annual 10<sup>th</sup>  
296 - 90<sup>th</sup> percentile range of 1.80) (Figure 3). A less consistent and coherent decrease in annual average  
297 concentrations in bulk precipitation was recorded for  $\text{NH}_4$  ( $R^2 = 0.58$  versus time,  $p < 0.001$ , mean  
298 annual 10<sup>th</sup> - 90<sup>th</sup> percentile range 1.94). Measured declines in  $\text{SO}_4$  concentrations were most  
299 pronounced during the 1990s whereas the  $\text{NO}_3$  concentration decrease was steepest after 2005 and  
300  $\text{NH}_4$  concentration has been decreasing linearly since 1994 (Figure 3).

301 The higher observed 10<sup>th</sup> - 90<sup>th</sup> percentile Z scores ranges for  $\text{NH}_4$  and  $\text{NO}_3$  concentration in bulk  
302 precipitation (compared to those observed for  $\text{SO}_4$ ) led us to test significance of the  $\text{NO}_3$  and  $\text{NH}_4$   
303 decrease in bulk precipitation at individual sites. For  $\text{NH}_4$  concentrations, significant ( $p < 0.05$ ; linear  
304 regression versus year) decreases in bulk precipitation were observed at 15 out of 30 sites. The  $\text{NO}_3$   
305 concentration significantly decreased at 22 sites ( $p < 0.05$ ; linear regression versus year) out of 30.  
306 Throughfall  $\text{NO}_3$  and  $\text{NH}_4$  concentrations were not included in the assessment. The absence of a  
307 significant overall change of throughfall DIN indicates that canopy N transformation plays a  
308 significant role in N delivery to the forest floor (Lovett and Lindberg 1993; Kopáček et al. 2009) and  
309 was more or less independent of actual N deposition level over the short to medium term.

310

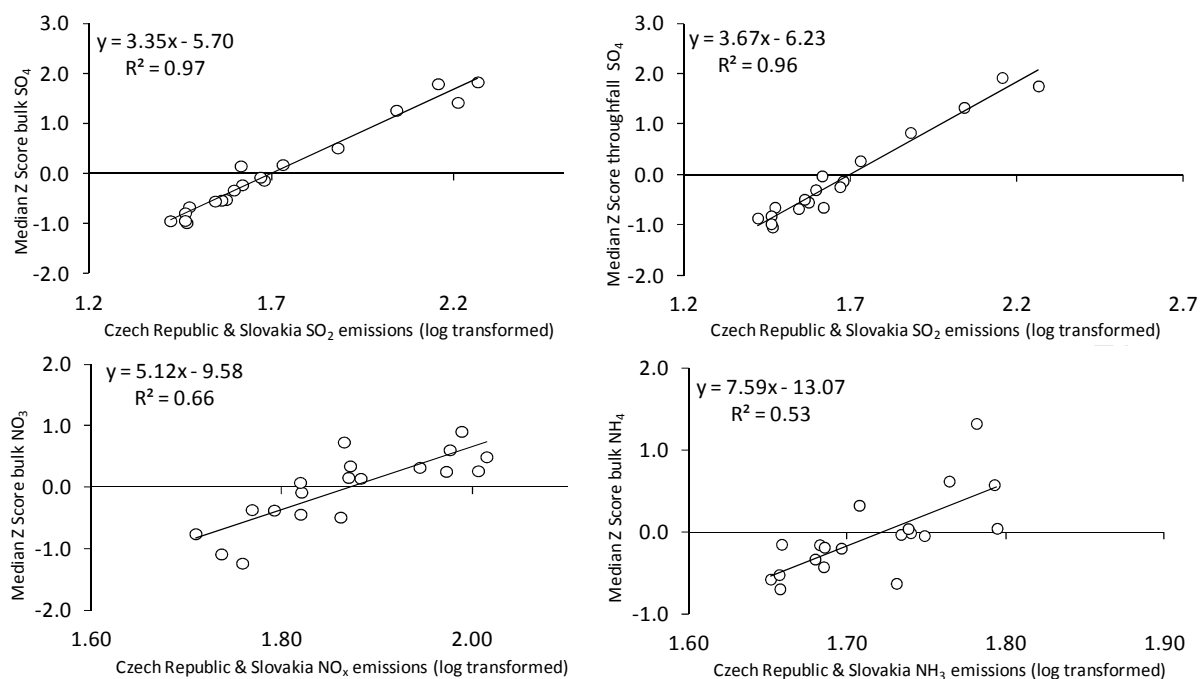


311  
 312 Figure 3. Standardised annual mean (Z score) time series for bulk and throughfall SO<sub>4</sub>, bulk NO<sub>3</sub> and  
 313 NH<sub>4</sub> concentrations for sites listed in Table S1. Bold central line shows median annual Z score for all  
 314 sites, outer lines show 10<sup>th</sup> and 90<sup>th</sup> percentile values. Dashed lines show linear regressions between  
 315 median annual Z scores and time.

## 316 3.2 ESTIMATION OF MEASURED HISTORICAL SO<sub>4</sub>, NH<sub>4</sub> AND NO<sub>3</sub> CONCENTRATIONS

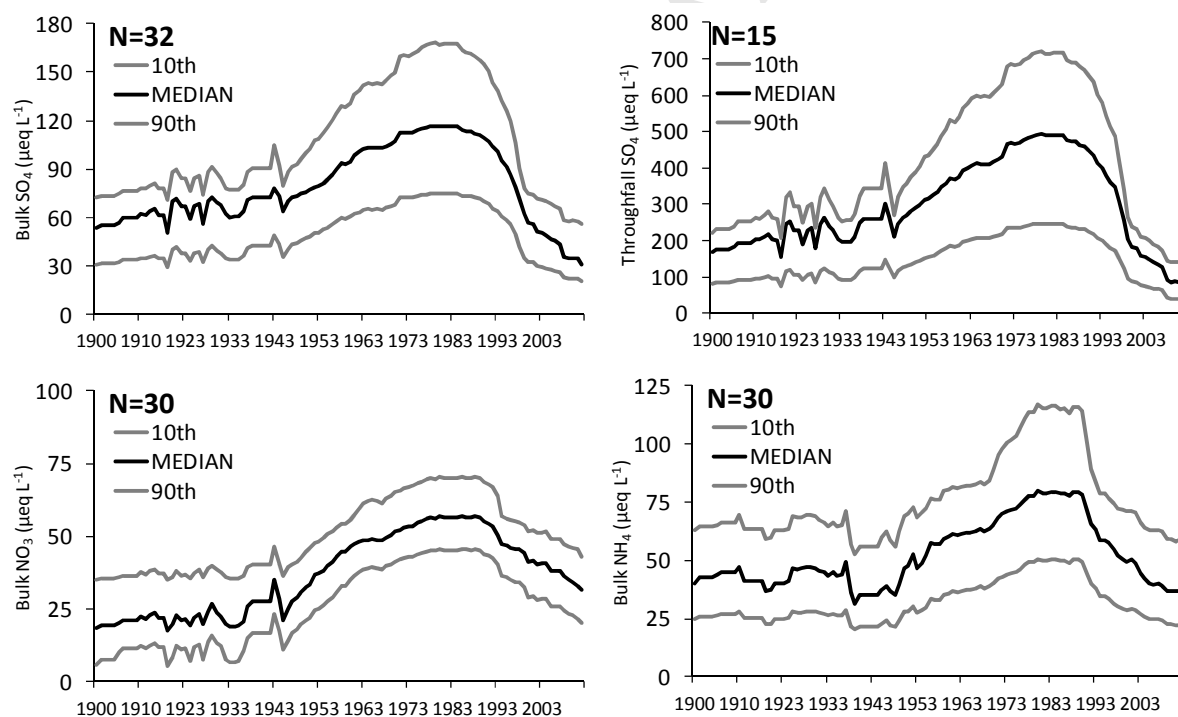
### 317 3.2.1 Reconstruction of SO<sub>4</sub> precipitation concentrations

318  
 319 The high degree of overall temporal coherence observed among sites in annual mean precipitation  
 320 SO<sub>4</sub> as well as throughfall SO<sub>4</sub> concentrations, and to a lesser extent precipitation NO<sub>3</sub> and NH<sub>4</sub>  
 321 concentrations, allowed the use of standardised median concentration as a representative measure  
 322 of change in respect of emission rates. For SO<sub>4</sub> in bulk precipitation, a strong relationship with log  
 323 transformed SO<sub>2</sub> emission rate was found ( $R^2 = 0.97$ ,  $p < 0.001$ ; Figure 4). According to this log-linear  
 324 regression equation, annual median SO<sub>4</sub> Z scores for precipitation were calculated from emission  
 325 rates for the whole period of emissions reconstruction (1900 - 2012). Modelled SO<sub>4</sub> concentration  
 326 (Figure 5) was compared with measured data across all years (including measurements before 1994)  
 327 and sites. Prediction of SO<sub>4</sub> had RMSE values ranging from 5.6 to 31  $\mu\text{eq L}^{-1}$  at individual sites (10<sup>th</sup>  
 328 and 90<sup>th</sup> percentile), with a median of 12.3  $\mu\text{eq L}^{-1}$  (20 % of median SO<sub>4</sub> concentration) across all sites  
 329 and years. Explained variability in the measured SO<sub>4</sub> concentration ranged between 41 % and 94 %,  
 330 with a median of 81 %. NSCD ranged between 0.32 and 0.92 with a median of 0.73 (Figure 6).  
 331 Similar results were obtained for throughfall SO<sub>4</sub> (Figure 5). The standardised Z score of SO<sub>4</sub>  
 332 throughfall was tightly related to the log transformed SO<sub>2</sub> emissions ( $R^2 = 0.96$ ,  $p < 0.001$ ; Figure 4).  
 333 Predicted RMSE of SO<sub>4</sub> throughfall varied between 18.5 and 87  $\mu\text{eq L}^{-1}$  (median 42  $\mu\text{eq L}^{-1}$ , which is  
 334 22% of median concentration across sites). Explained variability in the measured throughfall SO<sub>4</sub>  
 335 concentration ranged between 55 % and 97 %, with a median of 82 %. NSCD ranged between 0.51  
 336 and 0.94 with a median of 0.79 (Figure 6).  
 337



338  
 339 Figure 4. Linear regressions between median Z score of bulk and throughfall  $\text{SO}_4$ , bulk  $\text{NO}_3$ , and bulk  
 340  $\text{NH}_4$  and the CS emission rates (log transformed  $\text{mmol m}^{-2} \text{yr}^{-1}$ ) of the respective S and N compounds.

341



342  
 343 Figure 5. Modelled concentrations of bulk and throughfall  $\text{SO}_4$  and bulk  $\text{NO}_3$  and  $\text{NH}_4$ . Bold central  
 344 line shows median for all sites, outer lines show 10<sup>th</sup> and 90<sup>th</sup> percentile values.

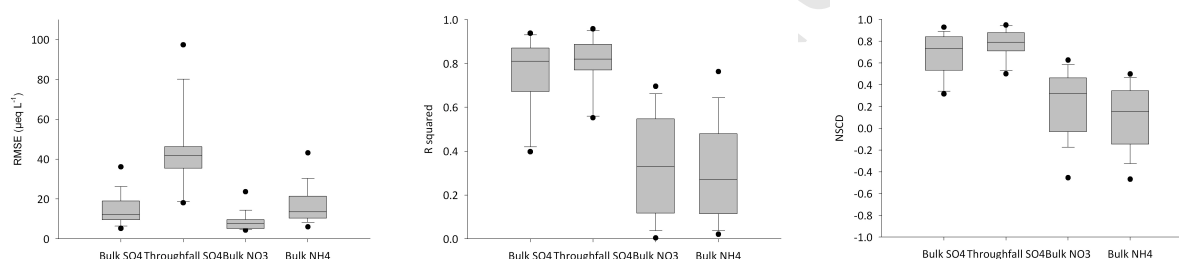
### 345 3.2.2 Reconstruction of $\text{NO}_3$ and $\text{NH}_4$ precipitation concentrations

346  
 347 For  $\text{NO}_3$ , a significant relationship ( $R^2 = 0.66$ ,  $p < 0.001$ ) between median Z score and log transformed  
 348  $\text{NO}_x$  emissions was observed (Figure 4). Variation of  $\text{NO}_3$  RMSE was between 4.5 and 19  $\mu\text{eq L}^{-1}$   
 349 (median 7.5  $\mu\text{eq L}^{-1}$ , which is 18 % of median concentration across sites). Explained variability in the  
 350 measured  $\text{NO}_3$  concentration ranged between 2 % and 68 %, with a median of 33 %. NSCD ranged

351 between -0.38 and 0.61 with a median of 0.32 (Figure 6). There was no obvious relationship between  
 352 model performance and site location. For  $\text{NH}_4$ , a weaker but still significant relationship ( $R^2 = 0.53$ ,  $p$   
 353  $< 0.01$ ) between median Z score and log transformed  $\text{NH}_3$  emissions was found (Figure 4). The RMSE  
 354 of modelled  $\text{NH}_4$  ranged between 7.1 and 41  $\mu\text{eq L}^{-1}$ , with median of 13.5  $\mu\text{eq L}^{-1}$  (28 % of median  
 355 concentration across sites). Explained variability in the measured  $\text{NH}_4$  concentration ranged between  
 356 3 % and 73 %, with a median of 27 %. NSCD ranged between -0.42 and 0.48 with a median of 0.16  
 357 (Figure 6).

358 The somewhat poorer correlations between  $\text{NH}_4$  and  $\text{NO}_3$  concentrations in precipitation and their  
 359 respective emissions compared to those observed for  $\text{SO}_4$  are probably caused by a higher degree of  
 360 year-to-year variability in the  $\text{NH}_4$  concentration in precipitation, as well as higher degree of inter site  
 361 trend heterogeneity as demonstrated in section 3.1. Moreover, components of  $\text{NO}_x$  ( $\text{NO}$  and  $\text{NO}_2$ ) are  
 362 much more reactive than  $\text{SO}_2$ , and therefore the atmospheric chemistry associated with  $\text{NO}_x$  is more  
 363 complex than for  $\text{SO}_2$  (Seinfeld and Pandis, 1998). The non-linearity between  $\text{NO}_x$  emissions and  
 364 precipitation concentration may therefore be more strongly influenced by changes in other  
 365 atmospheric chemical constituents than the equivalent relationship between  $\text{SO}_2$  emissions and S  
 366 precipitation (Fagerli and Aas, 2008). A lack of significant temporal changes in bulk nitrogen  
 367 deposition was confirmed for Sweden (Pihl Karlsson et al., 2011) and for the UK (Kernan et al., 2010).  
 368 On the other hand, significant correlations between precipitation concentration and emissions were  
 369 found in the eastern USA for both  $\text{NO}_x$  and  $\text{SO}_2$  (Butler et al., 2005; Likens et al., 2001).

370



371 Figure 6. Box plots showing distribution of statistical results for root mean square error (RMSE),  
 372 coefficient of determination ( $R^2$ ), and Nash-Sutcliffe coefficient of determination (NSCD) obtained for  
 373 individual sites. Median, 25<sup>th</sup> and 75<sup>th</sup> percentiles, whiskers indicate 5<sup>th</sup> and 95<sup>th</sup> percentiles and  
 374 minimum maximum values are denoted with dots.

375

### 376 3.2.3 Precipitation $\text{SO}_4$ , $\text{NO}_3$ and $\text{NH}_4$ concentrations during the peak of acid deposition

377

378 The non-linear relationships between standardised  $\text{SO}_4$ ,  $\text{NH}_4$  and  $\text{NO}_3$  concentrations and their  
 379 respective emissions were highlighted when long-term precipitation data (measurements from 1970s  
 380 and 1980s) were used for comparison (Figure S3). Such a dataset was available for the ANE, JEZ, LIZ,  
 381 NAC, SLA and PCJ for the period 1978-2012. This period covered the peak of emissions reported for  
 382 central Europe (Figure 1). Taking into account that CS emissions of  $\text{SO}_2$  and  $\text{NO}_x$  were  
 383 disproportionately higher during this period than for central Europe as a whole (Figure 1), the  
 384 balance of “emission export” from CS minus “emission import” from surrounding countries was  
 385 higher during the 1980s and 1990s than currently. On the other hand,  $\text{NH}_3$  emissions were  
 386 significantly lower in CS than in surrounding countries, probably leading to a net import. Log  
 387 transformation appears to correct for the discrepancy between CS and central European emissions,  
 388 by reducing modelled deposition estimates during the peak of CS emissions, leading to more  
 389 accurate fit between observed precipitation chemistry and emission rates. In future, it is expected  
 390 that further reductions in emissions should be followed by more linear responses in precipitation  
 391 concentrations. Similarly, long-term (1965 - 2000) precipitation monitoring at Hubbard Brook  
 392 Experimental Forest in U.S. showed non-significant relationships between  $\text{SO}_4$  bulk precipitation

393 concentrations and SO<sub>2</sub> emissions during the 1965 - 1980 period. A clear strong curvilinear  
 394 relationship was apparent only for the whole period 1965 - 2000 (Likens et al., 2005), again  
 395 suggesting a weaker relationship between concentration and emission during the period of peak SO<sub>2</sub>  
 396 emissions.

397

### 398 **3.3 SPATIAL ESTIMATION OF PRECIPITATION CHEMISTRY AT UNMONITORED SITES**

399

#### 400 **3.3.1 Spatial distribution of SO<sub>4</sub> concentrations in precipitation**

401

402 To calculate mean precipitation SO<sub>4</sub> concentration ( $C_{SO_4}$ ) all site characteristics (latitude, longitude,  
 403 precipitation and elevation) entered the regression model. All four predictors together explained 72  
 404 % of variability in the measured  $C_{SO_4}$  across 32 sites within the Czech Republic:

405

$$406 C_{SO_4} = 10^{(4.321 + 1.093 \times 10^{-4} \times E - 3.24 \times 10^{-4} \times P + 9.541 \times 10^{-7} \times Y + 1.607 \times 10^{-6} \times X)}$$

407

408 Latitude and longitude explained 40 % of variability and reflects a well known spatial gradient in  
 409 precipitation chemistry within the Czech Republic, due to the cluster of major emission sources in the  
 410 NW part of the country, i.e. a part of the former Black Triangle (Černý and Pačes, 1995). Annual  
 411 precipitation amount added 27 % of explained variability in the regression model – sites with higher  
 412 precipitation tend to have lower concentrations due to dilution effects. Tight coherence in  
 413 precipitation SO<sub>4</sub> trends across all sites (Figure 3) and fairly high explanatory power of the regression  
 414 model (72 %) led us to incorporate the modelled  $C_{SO_4}$  as next predictor for calculations of other  
 415 chemistry constituents (throughfall SO<sub>4</sub>, NO<sub>3</sub> and NH<sub>4</sub>).

416 The rate of change in precipitation SO<sub>4</sub> concentration ( $\Delta C_s$ ) was a function of  $C_{SO_4}$  (34 % of explained  
 417 variability), latitude (north-south gradient) and elevation.

418

$$419 \Delta C_{SO_4} = 1.927 - 9.317 \times 10^{-4} \times E - 5.639 \times \log(C_{SO_4}) - 5.048 \times 10^{-6} \times X$$

420

421 Relatively higher annual decreases in bulk SO<sub>4</sub> concentration were modelled for northern sites with  
 422 higher SO<sub>4</sub> concentrations (Figure S4). All together 44 % of variability in  $\Delta C_s$  was explained. Site  
 423 standard deviation ( $\sigma_{SO_4}$ ) was then calculated based on tight relationship between  $\sigma$  and  $\Delta C_s$   
 424 (Figure S2):

425

$$426 \sigma_{SO_4} = -6.24 \times \Delta C_{SO_4} + 1.57 \quad (R^2 = 0.92)$$

427

428 Model performance is highlighted in Figure 7. Modelled RMSE values were 16 % of site average value  
 429 for  $C_{SO_4}$ , 32 % of site mean change for modelled  $\Delta C_{SO_4}$ , and 34 % of mean site standard deviation for  
 430 modelled  $\sigma_{SO_4}$ .

431 Mean throughfall SO<sub>4</sub> concentration ( $C_{SO_4thf}$ ) across 15 sites with available data was best explained  
 432 with three predictors ( $C_{SO_4}$ , precipitation and latitude).

433

$$434 C_{SO_4thf} = 10^{(1.557 + 1.165 \times \log(C_{SO_4}) - 3.57 \times 10^{-4} \times P + 8.941 \times 10^{-7} \times X)}$$

435

436 All together 90 % of the variability in  $C_{SO_4thf}$  was explained, from which 73 % was related to the  
 437 respective bulk SO<sub>4</sub> concentration. Thus, sites with high SO<sub>4</sub> concentration in precipitation tend to  
 438 have high throughfall (Figure 8). Rate of change in throughfall SO<sub>4</sub> concentration ( $\Delta C_{SO_4thf}$ ) was a  
 439 function of  $C_{SO_4thf}$  (83 % of explained variability) and longitude (Figure S4).

440

$$441 \Delta C_{SO_4thf} = 43.263 - 23.581 \times \log(C_{SO_4thf}) + 8.399 \times 10^{-6} \times Y$$

442

443 Sites located in the west and with high throughfall SO<sub>4</sub> concentrations experienced the steepest  
 444 declines in throughfall SO<sub>4</sub> concentration. Altogether 86 % of the variability in  $\Delta C_{SO_4thf}$  was explained  
 445 by  $C_{SO_4thf}$  and longitude. Site standard deviation ( $\sigma_{SO_4thf}$ ) was then calculated according to linear  
 446 regression from the Figure S2:

$$447$$

$$448 \sigma_{SO_4thf} = -6.83 \times \Delta C_{SO_4thf} - 2.35 \quad (R^2=0.98)$$

$$449$$

450 Modelled RMSE values were 26 % of site average value for  $C_{SO_4thf}$ , 19 % of site mean change for  
 451 modelled  $\Delta C_{SO_4thf}$ , and 21 % of mean site standard deviation for modelled  $\sigma_{SO_4thf}$  (Figure 7).

452

### 453 3.3.2 Spatial distribution of NO<sub>3</sub> and NH<sub>4</sub> concentrations in precipitation

454

455 Mean precipitation NO<sub>3</sub> concentration ( $C_{NO_3}$ ) across 30 sites with available data was best explained  
 456 with two predictors:

457

$$458 C_{NO_3} = 10^{(1.123 + 5.156 \times 10^{-3} \times C_{SO_4} - 2.643 \times 10^{-7} \times Y)}$$

459

460 Mean bulk SO<sub>4</sub> concentration explained 49 % in variation of mean bulk NO<sub>3</sub> concentration, another  
 461 12 % of explanatory power added longitude. Sites with high SO<sub>4</sub> concentration in the west part of the  
 462 territory tend to have higher NO<sub>3</sub> concentration in bulk precipitation (Figure 8). This further reflects  
 463 importance of the proximity from large stationary sources of NO<sub>x</sub> emissions that dominated NO<sub>x</sub>  
 464 emissions in the Czech Republic in the 1980s and 1990s (Kopacek and Vesely, 2005).

465 Absolute change in the NO<sub>3</sub> concentration was related to latitude (14 % of explained variability in  
 466  $\Delta C_{NO_3}$ ), precipitation and elevation. All together 36 % of variability in  $\Delta C_{NO_3}$  was explained.

467

$$468 \Delta C_{NO_3} = -4.687 - 8.589 \times 10^{-4} \times E + 4.515 \times 10^{-4} \times P - 3.775 \times 10^{-6} \times X$$

469

470 Higher decreases were observed in northern sites (Figure S4). Site standard deviation ( $\sigma_{NO_3}$ ) was  
 471 then calculated based on linear regression from the Figure S2.

472

$$473 \sigma_{NO_3} = -5.35 \times \Delta C_{NO_3} + 3.44$$

474

475 Compared to SO<sub>4</sub> assessment, predictive performance of regression models were poorer, with the  
 476 modelled RMSE values of 15 % of site average value for  $C_{NO_3}$ , 36 % of site mean change for modelled  
 477  $\Delta C_{NO_3}$ , and 29 % of mean site standard deviation for modelled  $\sigma_{NO_3}$  (Figure 7).

478 Mean precipitation NH<sub>4</sub> concentration ( $C_{NH_4}$ ) across 30 sites with available data was best explained  
 479 with four predictors.

480

$$481 C_{NH_4} = 10^{(0.316 - 6.733 \times 10^{-5} \times P + 7.505 \times 10^{-3} \times C_{SO_4} - 4.950 \times 10^{-7} \times Y - 6.026 \times 10^{-7} \times X)}$$

482

483 Bulk SO<sub>4</sub> concentration alone explained 58 % of  $C_{NH_4}$  variability across sites,  
 484 precipitation added 12 % to explained variability and 8 % was explained by the  
 485 coordinates.  $C_{NH_4}$  tends to be higher at sites with high SO<sub>4</sub> concentration,  
 486 reflecting the role of NH<sub>4</sub> as a counter-ion to SO<sub>4</sub> in (NH<sub>4</sub>)<sub>2</sub>SO<sub>4</sub> aerosol.  
 487 Furthermore, in contrast to NO<sub>3</sub>, NH<sub>4</sub> tends to be higher in the SW territory of  
 488 the Czech Republic (Figure 8). This is in good spatial agreement with the  
 489 distribution of industrial and agricultural areas across the Czech Republic,  
 490 as well as with closer proximity of NH<sub>3</sub> emission sources in Germany that are  
 491 higher than the CS sources (EMEP; [www.ceip.at/emission-data-webdab](http://www.ceip.at/emission-data-webdab)) due to  
 492 higher density of livestock production (FAO; <http://faostat.fao.org>).

493 The concentration change was related to  $C_{SO_4}$  (29 % of explained variability) and to precipitation and  
 494 elevation. Overall, 45 % of annual change in NH<sub>4</sub> concentration was explained.

495

496 
$$\Delta C_{\text{NH}_4} = 0.413 - 1.334 \times 10^{-3} \times E + 1.075 \times 10^{-3} \times P - 3.279 \times 10^{-2} \times C_{\text{SO}_4}$$

497

498 The steepest decline tends to be at sites with highest  $\text{SO}_4$  concentrations (Figure S4). Site standard  
499 deviation ( $\sigma_{\text{NH}_4}$ ) was then calculated based on the linear regression from the Figure S2.

500

501 
$$\sigma_{\text{NH}_4} = -5.59 \times \Delta C_{\text{NH}_4} + 7.2$$

502

503 Modelled mean  $C_{\text{NH}_4}$  RMSE was 25 % of site average value, modelled  $\Delta C_{\text{NH}_4}$  RMSE was 56 % of site  
504 mean change and modelled  $\sigma_{\text{NH}_4}$  RMSE was 39 % of mean site standard deviation (Figure 7).

505 Concentrations of inorganic nitrogen were less satisfactorily predicted than  $\text{SO}_4$  concentrations in

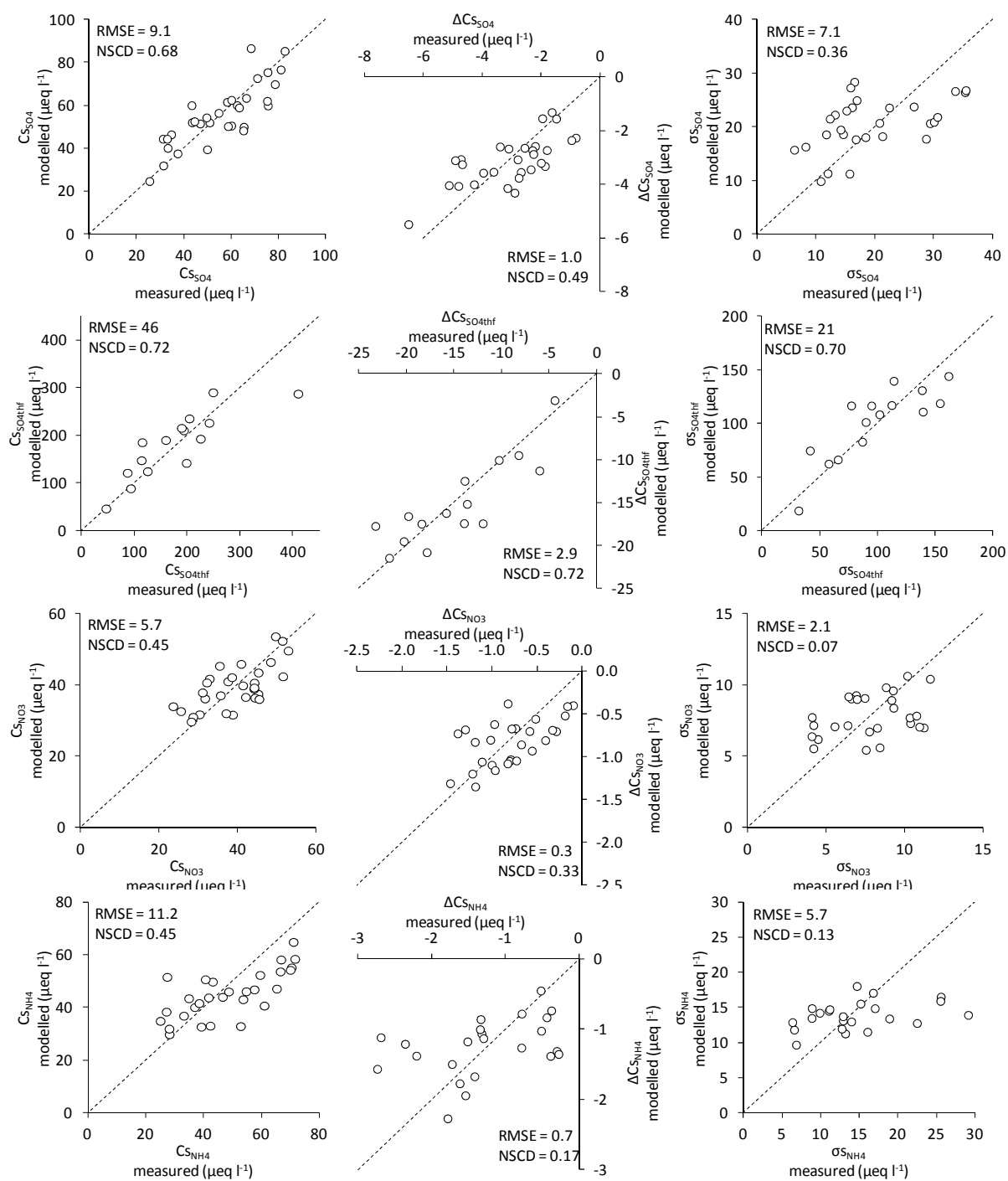
506 precipitation. Related to the previous discussion, higher degree of year-to-year variability in the N

507 concentration in precipitation and higher degree of inter site trend heterogeneity caused poorer

508 performance of regression models compared to the well constrained trends in  $\text{SO}_4$  concentrations.

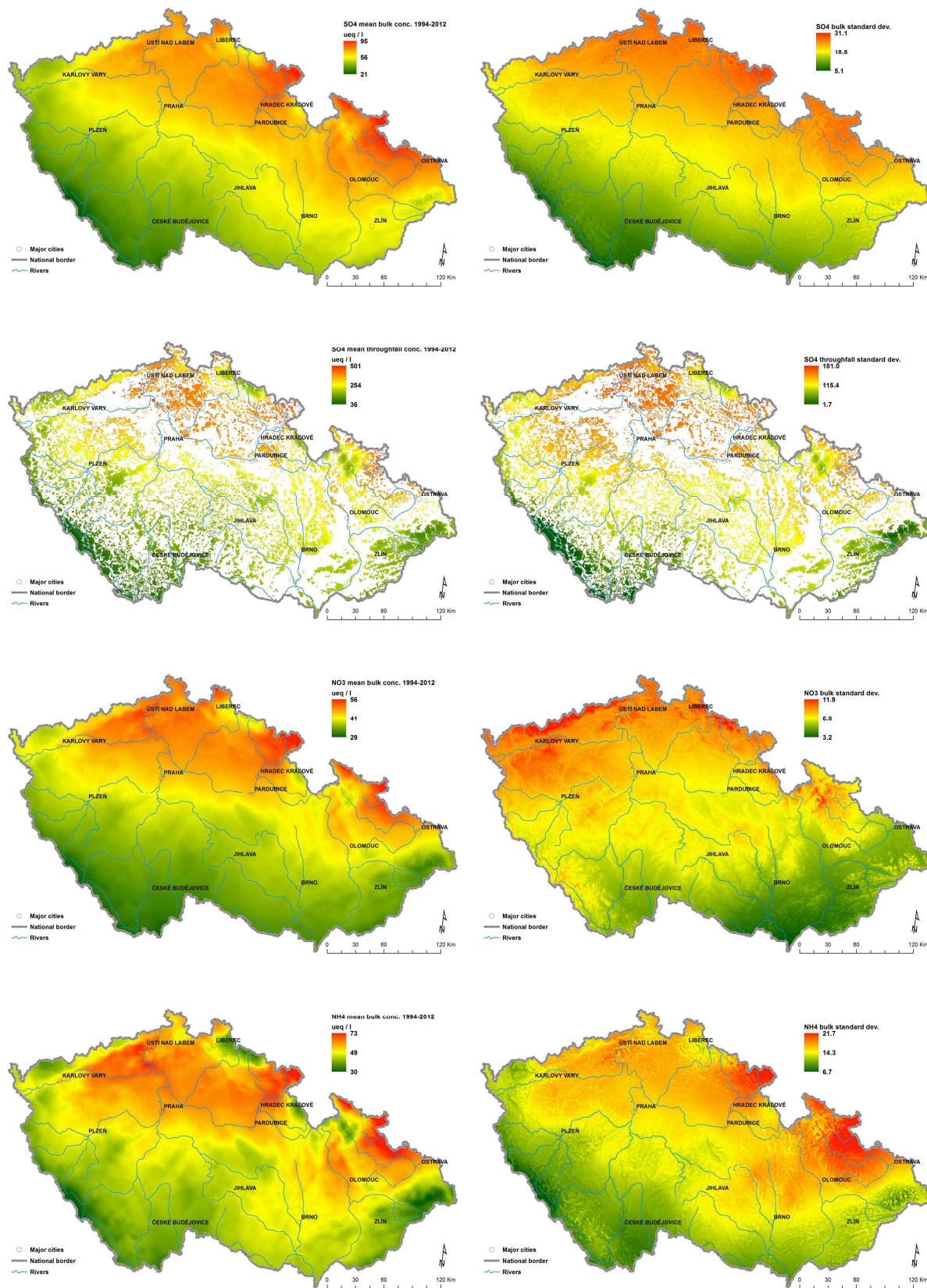
509 However, calculated spatial distribution of precipitation chemistry ( $C_s$ ,  $\sigma_s$ ) can be used to estimate

510 historical deposition gradients across the Czech Republic.



511  
 512 Figure 7. 1:1 plots of modelled vs. measured mean SO<sub>4</sub>, NO<sub>3</sub> and NH<sub>4</sub> concentrations (Cs) at the study  
 513 sites, annual rate of change (ΔCs), site standard deviation (σs). Root mean square error (RMSE) and  
 514 Nash-Sutcliffe coefficient of determination (NSCD) are displayed.





515  
516 Figure 8. Spatial distribution of calculated mean Cs and os across the Czech Republic.

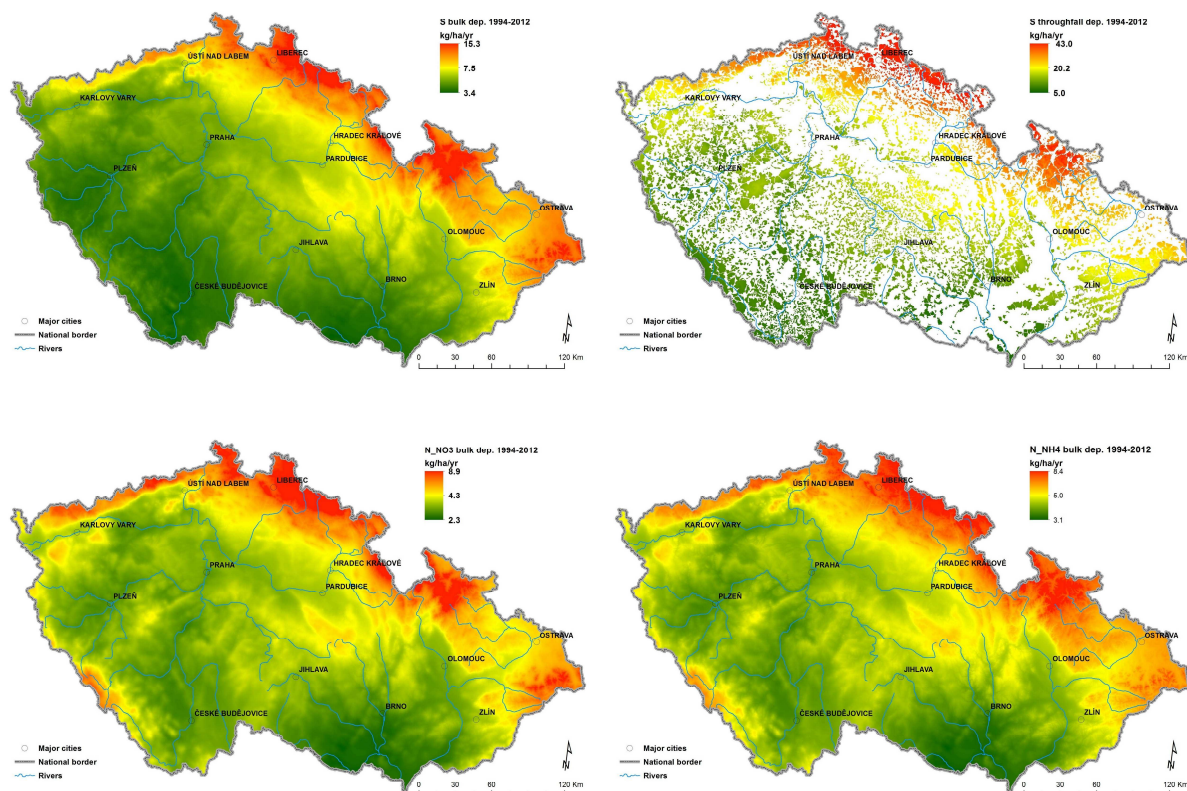
## 518 **3.4 SPATIAL ESTIMATION OF S AND N DEPOSITION ACROSS THE CZECH REPUBLIC** 519 **BETWEEN 1900 AND 2012** 520

### 521 **3.4.1 Temporal development of S deposition** 522

523 Estimated average S bulk deposition across the Czech Republic was a product of the spatial  
524 distribution of modelled  $C_{S_{SO_4}}$  and mean precipitation depth. Highest S bulk deposition was modelled  
525 for northern part of the Czech Republic, especially in the mountainous landscape. For the calibration  
526 period (1994 - 2012), average S bulk deposition ranged between 3.5 and 15 kg S ha<sup>-1</sup> yr<sup>-1</sup> across the  
527 Czech Republic (Figure 9). Over the 20<sup>th</sup> century, estimated median S bulk deposition increased from  
528 5 kg S ha<sup>-1</sup> yr<sup>-1</sup> (1900) to 11.6 kg S ha<sup>-1</sup> yr<sup>-1</sup> (1979) and then declined to 3.8 kg S ha<sup>-1</sup> yr<sup>-1</sup> (2012) (Figure  
529 S5). Current S bulk deposition is thus lower than estimated deposition in 1900. Between peak of the  
530 bulk S deposition and the year 2012, deposition declined by 67 %. Between 1979 and 2012, the rate  
531 of decline in bulk S deposition ( $\Delta C_{S_{SO_4}}$ ) ranged between -0.19 and -0.48 kg S ha<sup>-1</sup> yr<sup>-1</sup> (median of -0.29  
532 kg S ha<sup>-1</sup> yr<sup>-1</sup>) (Figure S4). Over the 20<sup>th</sup> century (1900 – 2012) cumulative CS (Czechoslovakia area  
533 based) SO<sub>2</sub> emissions were on average ~5025 kg S ha<sup>-1</sup> and the modelled bulk S deposition (for the  
534 same area) was 945 kg S ha<sup>-1</sup> for the same period.

535 Forests in the Czech Republic cover ca. 34 % of country area and consist mainly of production forests  
536 (75 %) with predominantly conifer species (73 %). During the 20<sup>th</sup> century forest area increased by ca.  
537 5 %. Because canopy exchange of S is negligible, higher throughfall versus bulk deposition can be  
538 attributed to dry S deposition, such that throughfall provides a good measure of the total  
539 atmospheric deposition of S (Lindberg and Lovett, 1992). Average S throughfall (total) deposition was  
540 highest in the northern part of the Czech Republic, with the highest estimated deposition in the  
541 mountain areas. Between 1994 and 2012, average S total deposition under the spruce canopy ranged  
542 between 5 and 43 kg S ha<sup>-1</sup> yr<sup>-1</sup> (Figure 9). Over the 20<sup>th</sup> century, estimated country median S total  
543 deposition increased from 14 kg S ha<sup>-1</sup> yr<sup>-1</sup> (1900) to 41 kg S ha<sup>-1</sup> yr<sup>-1</sup> (1979) and then declined to 7.3  
544 kg S ha<sup>-1</sup> yr<sup>-1</sup> (2012) (Figure S5). Between peak of the S total deposition and year 2012, the throughfall  
545 S deposition declined by 82 %, i.e. faster than bulk S deposition. Between 1979 and 2012 the rate of  
546 decline in total S deposition ( $\Delta C_{S_{SO_4thf}}$ ) ranged between -0.9 and -2.3 kg S ha<sup>-1</sup> yr<sup>-1</sup> (median of -1.3 kg S  
547 ha<sup>-1</sup> yr<sup>-1</sup>). The most pronounced decline in S total deposition was modelled for forests close to the  
548 biggest stationary SO<sub>2</sub> sources (mostly brown coal burning powerplants) in the NW part of the Czech  
549 Republic (Figure S4)(Hůnová et al., 2014). On average, cumulative S deposition in Czech forests is  
550 estimated to be 3048 kg S ha<sup>-1</sup> during the 20<sup>th</sup> century. In total, due to the majority of non-forested  
551 landscape (66 %) with relatively low dry deposition on vegetation surfaces, 34 % of emitted S in the  
552 Czech Republic has been deposited within its own territory as bulk or throughfall deposition since  
553 1900. Currently, 70 % of Czech SO<sub>2</sub> emissions is deposited within the country boundaries. However,  
554 during the peak of SO<sub>2</sub> pollution, 20 % of emitted S in the Czech Republic has been deposited within  
555 its own territory.

556 Based on the analysis, enrichment of throughfall deposition over the bulk deposition (DDF – dry  
557 deposition factor) varied between 1.7 and 6.6, with the highest ratio in the NW of the Czech  
558 territory. Again, sites closest to the S emission sources had the highest DDF (Figure 10). Over the last  
559 hundred years, median DDF peaked in the 1980s at 3.4 (10<sup>th</sup> and 90<sup>th</sup> percentile range of 2.9 and 3.8)  
560 and declined to 1.7 in 2012 (10<sup>th</sup> and 90<sup>th</sup> percentile range between 1 and 2.6) (Figure S5).  
561

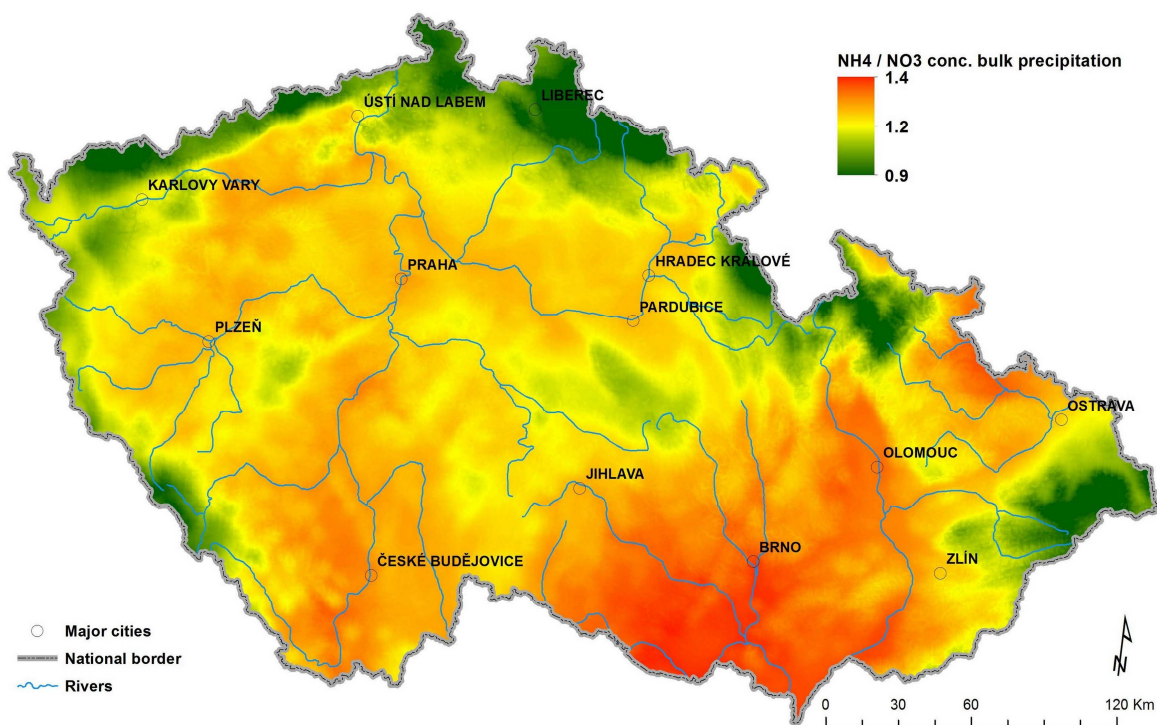
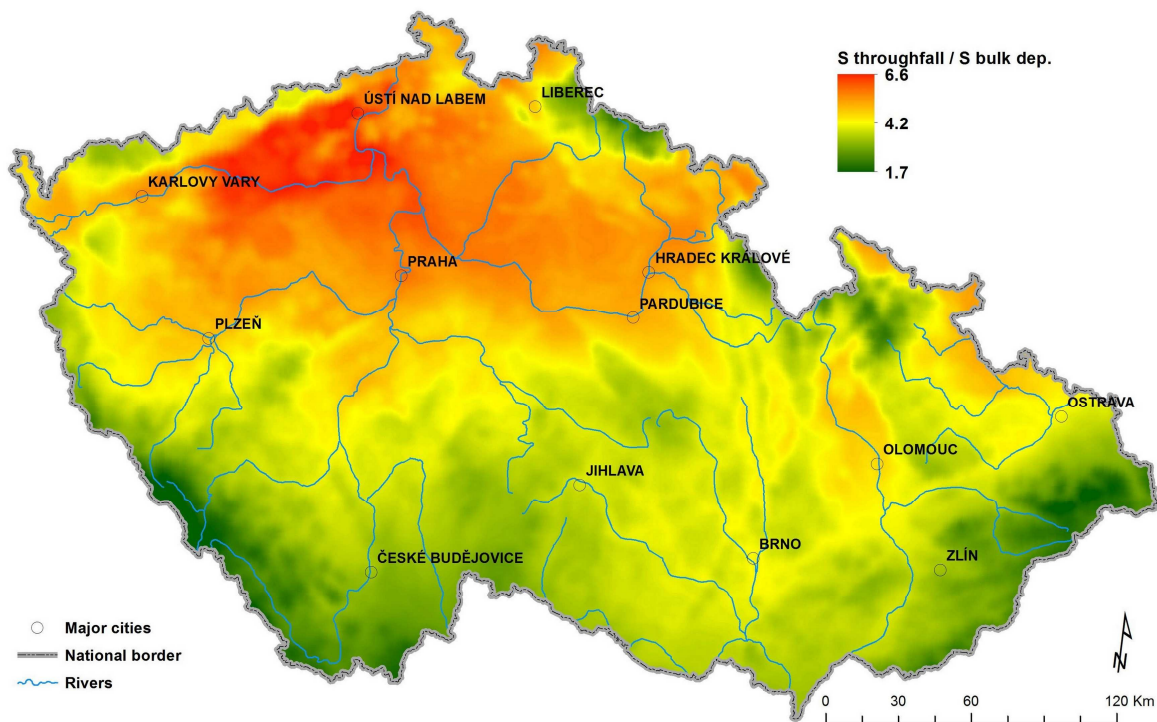


562  
563 Figure 9. Modelled average deposition ( $\text{kg ha}^{-1} \text{yr}^{-1}$ ) of S (bulk and throughfall) and N (bulk)  
564 compounds in the Czech Republic during 1994–2012.

### 565 3.4.2 Temporal development of N deposition

566  
567 Spatial distribution of both  $\text{NO}_3$  and  $\text{NH}_4$  bulk concentration was statistically related to  $\text{SO}_4$   
568 concentration in precipitation. Although modelled  $\text{Cs}_{\text{SO}_4}$  as a predictor of spatial distribution of  $\text{Cs}_{\text{NO}_3}$   
569 and  $\text{Cs}_{\text{NH}_4}$  may induce additional error in regression modelling, both N species concentrations were  
570 statistically related to the  $\text{SO}_4$ , likely reflecting common sources ( $\text{SO}_2$  and  $\text{NO}_x$  emissions) or/and  
571 linked atmospheric chemistry ( $\text{SO}_4$  and  $\text{NH}_4$ ). Modelled deposition of  $\text{NO}_3$  was highest in the  
572 mountain areas across the Czech Republic, with a south – north gradient. The average  $\text{NO}_3$  deposition  
573 ranged between 2.3 and 8.9  $\text{kg N-NO}_3 \text{ ha}^{-1} \text{yr}^{-1}$  from 1994 – 2012 (Figure 9). Bulk  $\text{NO}_3$  deposition was  
574 2.4  $\text{kg N ha}^{-1} \text{yr}^{-1}$  in 1900, which is lower than its current level. The peak of  $\text{NO}_3$  deposition occurred in  
575 1988, with a median value of 5.3  $\text{kg N ha}^{-1} \text{yr}^{-1}$ . Since then,  $\text{NO}_3$  deposition declined by 38 % to 3.3  $\text{kg N}$   
576  $\text{ha}^{-1} \text{yr}^{-1}$  (Figure S5). The median decline was calculated as  $-0.07 \text{ kg N ha}^{-1} \text{yr}^{-1}$  (range between  $-0.05$   
577 and  $-0.11 \text{ kg N ha}^{-1} \text{yr}^{-1}$ ). The most pronounced declines in  $\text{NO}_3$  deposition were modelled for western  
578 and north-western part of the Czech Republic (Figure S4). Cumulative  $\text{NO}_3$  deposition over the 1900–  
579 2012 period was 409  $\text{kg N ha}^{-1}$ , which accounted for 33 % of the emissions of oxidized N forms.  
580 The modelled spatial distribution of ammonium deposition was similar to  $\text{NO}_3$ , with less deposition in  
581 the eastern part of the Czech Republic. The average  $\text{NH}_4$  deposition ranged between 3.1 and 8.4  $\text{kg N}$   
582  $\text{ha}^{-1} \text{yr}^{-1}$  (Figure 9). Bulk  $\text{NH}_4$  deposition was 4.2  $\text{kg N ha}^{-1} \text{yr}^{-1}$  in 1900, i similar to its current  
583 deposition (Figure S5), and peaked in 1984 with a median of 7.2  $\text{kg N ha}^{-1} \text{yr}^{-1}$ . Since then,  $\text{NH}_4$   
584 deposition declined by 46 % to 3.9  $\text{kg N ha}^{-1} \text{yr}^{-1}$ . Modelled decline ranged between  $-0.11$  and  $-0.2 \text{ kg N}$   
585  $\text{ha}^{-1} \text{yr}^{-1}$  (median of  $-0.14 \text{ kg N ha}^{-1} \text{yr}^{-1}$ ). The most pronounced declines occurred in northern and  
586 north-eastern parts of the country (Figure S4). Cumulative  $\text{NH}_4$  deposition was estimated to 576  $\text{kg N}$   
587  $\text{ha}^{-1}$  during 1900 – 2012, which accounted for 62 % of the CS emissions of  $\text{NH}_3$ . Spatially distributed  
588  $\text{NO}_3$  and  $\text{NH}_4$  precipitation concentrations reflects the nature of country land use, with higher  $\text{NH}_4$  to  
589  $\text{NO}_3$  ratios in lowland, agricultural landscapes (Figure 10). Temporal development of the  $\text{NH}_4$  to  $\text{NO}_3$

590 ratio in precipitation reflects different temporal changes in energy production (sources and amount)  
591 and agricultural activities (mostly livestock production) (Kopáček and Veselý, 2005). Two distinct  
592 period of time highlight those changes – after the 2nd World War and then after the political changes  
593 in 1989 (Figure S5) (Kopáček et al., 2013).



595 Figure 10. Mean modelled ratio between throughfall and bulk S deposition and  $\text{NH}_4$  to  $\text{NO}_3$  molar  
596 ratio in bulk precipitation in the Czech Republic in the period 1994 – 2012.

597

## 598 **4 CONCLUSIONS**

---

599

600 The methodology described in this paper represents a novel approach to the temporal  
601 reconstruction and spatial interpolation of atmospheric deposition chemistry, based on a simple  
602 statistical analysis of precipitation and throughfall monitoring data. Standardisation of precipitation  
603 chemistry to annual mean Z scores provides a robust method for comparing sites with different levels  
604 of absolute concentrations, and relationships between these Z scores and regional S and N emissions  
605 enabled us to reconstruct long-term changes in total deposition at the scale of the Czech Republic for  
606 the entire 20<sup>th</sup> century. Empirically-based interpolation, taking into account of key variables such as  
607 altitude, precipitation depth and geographical coordinates, allowed spatial variations in deposition to  
608 be mapped at a high resolution based on just 30 monitoring sites. The combination of temporal  
609 extrapolation and spatial interpolation allowed us to generate whole-country S and N budgets for the  
610 Czech Republic, which indicate that the country has undergone a transition from a strong net  
611 exporter of S to one in which the majority of (much lower) S emissions are now redeposited within  
612 the country.

613 Our results demonstrate that long-term measurements of atmospheric deposition, in combination  
614 with a statistical method that exploits observed spatio-temporal coherence in deposition chemistry,  
615 provides a robust approach for upscaling the observed data to other locations. As an important  
616 anthropogenic driver in many regions, the capacity to estimate site-specific S and N deposition over  
617 long time periods is a requirement for many models that seek to predict the historic and future  
618 trajectory of change in natural and semi-natural ecosystems, and a prerequisite for understanding  
619 the ecological changes that have occurred in many ecosystems affected by atmospheric pollution  
620 over the last 100 years.

621

### 622 **Acknowledgements**

623 Filip Oulehle and Tomáš Chuman acknowledge the Czech Science Foundation Grant no. 14-33311S.  
624 Further support was provided by the People Programme (Marie Curie Actions) of the EU 7FP under  
625 REA grant agreement no. PCIG13-GA-2013-618430 to Filip Oulehle. Jiří Kopáček and Petr Štěpánek  
626 acknowledge Science Foundation Grant no. P504/14/12262S. Additional support was provided by  
627 project CzechAdapt – System for Exchange of Information on Climate Change Impacts, Vulnerability  
628 and Adaptation Measures on the Territory of the Czech Republic (EHP-CZ02-OV-1-014-2014) which  
629 was supported by grant from Iceland, Liechtenstein and Norway. Furthermore, we would like to  
630 thank several partner organisations involved in supporting the continuation of the site monitoring.

631

632 **References**

- 633 Bobbink, R., Hicks, K., Galloway, J., Spranger, T., Alkemade, R., Ashmore, M., Bustamante, M.,  
634 Cinderby, S., Davidson, E., Dentener, F., Emmett, B., Erisman, J.W., Fenn, M., Gilliam, F., Nordin,  
635 A., Pardo, L., De Vries, W., 2010. Global assessment of nitrogen deposition effects on terrestrial  
636 plant diversity: a synthesis. *Ecol. Appl.* 20, 30–59.
- 637 Bonten, L.T.C., Reinds, G.J., Posch, M., 2016. A model to calculate effects of atmospheric deposition  
638 on soil acidification, eutrophication and carbon sequestration. *Environ. Model. Softw.* 79, 75–  
639 84. doi:10.1016/j.envsoft.2016.01.009
- 640 Butler, T., Likens, G., Vermeylen, F., Stunder, B., 2005. The impact of changing nitrogen oxide  
641 emissions on wet and dry nitrogen deposition in the northeastern USA. *Atmos. Environ.* 39,  
642 4851–4862. doi:10.1016/j.atmosenv.2005.04.031
- 643 Černý, J., Pačes, T. (Eds.), 1995. Acidification in the Black Triangle Region. Czech Geological Survey,  
644 Prague.
- 645 De Vries, W., Wamelink, G.W.W., van Dobben, H., Kros, J., Reinds, G.J., Mol-Dukstra, J.P., Smart, S.M.,  
646 Evans, C.D., Rowe, E.C., Belyazid, S., Sverdrup, H.U., van Hinsberg, A., Posch, M., Hettelingh, J.P.,  
647 Spranger, T., Bobbink, R., 2010. Use of dynamic soil-vegetation models to assess impacts of  
648 nitrogen deposition on plant species composition: an overview. *Ecol. Appl.* 20, 60–79.
- 649 Evans, C.D., Cooper, D.M., Monteith, D.T., Helliwell, R.C., Moldan, F., Hall, J., Rowe, E.C., Cosby, B.J.,  
650 2010. Linking monitoring and modelling: can long-term datasets be used more effectively as a  
651 basis for large-scale prediction? *Biogeochemistry* 101, 211–227. doi:10.1007/s10533-010-9413-  
652 x
- 653 Fagerli, H., Aas, W., 2008. Trends of nitrogen in air and precipitation: model results and observations  
654 at EMEP sites in Europe, 1980–2003. *Environ. Pollut.* 154, 448–61.  
655 doi:10.1016/j.envpol.2008.01.024
- 656 Hofmeister, J., Oulehle, F., Krám, P., Hruška, J., 2008. Loss of nutrients due to litter raking compared  
657 to the effect of acidic deposition in two spruce stands, Czech Republic. *Biogeochemistry* 88,  
658 139–151. doi:10.1007/s10533-008-9201-z
- 659 Hůnová, I., Maznová, J., Kurfürst, P., 2014. Trends in atmospheric deposition fluxes of sulphur and  
660 nitrogen in Czech forests. *Environ. Pollut.* 184, 668–75. doi:10.1016/j.envpol.2013.05.013
- 661 Janssen, P.H.M., Heuberger, P.S.C., 1995. Calibration of process-oriented models. *Ecol. Modell.* 83,  
662 55–66.
- 663 Kernan, M., Battarbee, R.W., Curtis, C., Monteith, D.T., Shilland, E.M., 2010. UK Acid Waters  
664 Monitoring Network 20 Year Interpretative Report. Report to DEFRA. London, UK.
- 665 Kopáček, J., Hejzlar, J., Posch, M., 2013. Factors Controlling the Export of Nitrogen from Agricultural  
666 Land in a Large Central European Catchment during 1900–2010. *Environ. Sci. Technol.* 47,  
667 130528133920004. doi:10.1021/es400181m
- 668 Kopáček, J., Posch, M., 2011. Anthropogenic nitrogen emissions during the Holocene and their  
669 possible effects on remote ecosystems. *Global Biogeochem. Cycles* 25, GB2017.  
670 doi:10.1029/2010GB003779
- 671 Kopáček, J., Posch, M., Hejzlar, J., Oulehle, F., Volková, A., 2012. An elevation-based regional model  
672 for interpolating sulphur and nitrogen deposition. *Atmos. Environ.* 50, 287–296.  
673 doi:10.1016/j.atmosenv.2011.12.017
- 674 Kopacek, J., Vesely, J., 2005. Sulfur and nitrogen emissions in the Czech Republic and Slovakia from

- 675 1850 till 2000. *Atmos. Environ.* 39, 2179–2188. doi:10.1016/j.atmosenv.2005.01.002
- 676 Kopacek, J., Vesely, J., Stuchlik, E., Kopáček, J., Veselý, J., Stuchlík, E., 2001. Sulphur and nitrogen  
677 fluxes and budgets in the Bohemian Forest and Tatra Mountains during the Industrial  
678 Revolution (1850-2000). *Hydrol. Earth Syst. Sci.* 5, 391–405.
- 679 Likens, G.E., Buso, D.C., Butler, T.J., 2005. Long-term relationships between SO<sub>2</sub> and NO<sub>x</sub> emissions  
680 and SO<sub>4</sub>(<sup>2-</sup>) and NO<sub>3</sub><sup>-</sup> concentration in bulk deposition at the Hubbard Brook Experimental  
681 Forest, NH. *J. Environ. Monit.* 7, 964–8. doi:10.1039/b506370a
- 682 Likens, G.E., Butler, T.J., Buso, D.C., 2001. Long-and short-term changes in sulfate deposition: Effects  
683 of the 1990 clean air act amendments. *Biogeochemistry* 52, 1–11.  
684 doi:10.1023/A:1026563400336
- 685 Lindberg, S., Lovett, G., 1992. Deposition and forest canopy interactions of airborne sulfur: Results  
686 from the integrated forest study. *Atmos. Environ. Part A. Gen. Top.* 26, 1477–1492.  
687 doi:10.1016/0960-1686(92)90133-6
- 688 Mylona, S., 1996. Sulphur dioxide emissions in Europe 1880-1991 and their effect on sulphur  
689 concentrations and depositions. *Tellus* 48B, 662–689.
- 690 Nash, J.E., Sutcliffe, J.V., 1970. River flow forecasting through conceptual models part I — A  
691 discussion of principles. *J. Hydrol.* 10, 282–290. doi:10.1016/0022-1694(70)90255-6
- 692 Oulehle, F., Cosby, B.J., Austnes, K., Evans, C.D., Hruška, J., Kopáček, J., Moldan, F., Wright, R.F., 2015.  
693 Modelling inorganic nitrogen in runoff: Seasonal dynamics at four European catchments as  
694 simulated by the MAGIC model. *Sci. Total Environ.* 536, 1019–28.  
695 doi:10.1016/j.scitotenv.2015.05.047
- 696 Oulehle, F., Evans, C.D., Hofmeister, J., Krejci, R., Tahovska, K., Persson, T., Cudlin, P., Hruska, J., 2011.  
697 Major changes in forest carbon and nitrogen cycling caused by declining sulphur deposition.  
698 *Glob. Chang. Biol.* 17, 3115–3129. doi:10.1111/j.1365-2486.2011.02468.x
- 699 Pihl Karlsson, G., Akselsson, C., Hellsten, S., Karlsson, P.E., 2011. Reduced European emissions of S  
700 and N—effects on air concentrations, deposition and soil water chemistry in Swedish forests.  
701 *Environ. Pollut.* 159, 3571–82. doi:10.1016/j.envpol.2011.08.007
- 702 Rogora, M., Mosello, R., Arisci, S., Brizzio, M.C., Barbieri, A., Balestrini, R., Waldner, P., Schmitt, M.,  
703 Stähli, M., Thimonier, A., Kalina, M., Puxbaum, H., Nickus, U., Ulrich, E., Probst, A., 2006. An  
704 Overview of Atmospheric Deposition Chemistry over the Alps: Present Status and Long-term  
705 Trends. *Hydrobiologia* 562, 17–40. doi:10.1007/s10750-005-1803-z
- 706 Schöpp, W., Posch, M., Mylona, S., Johansson, M., 2003. Long-term development of acid deposition  
707 (1880-2030) in sensitive freshwater regions in Europe. *Hydrol. Earth Syst. Sci.* 7, 436–446.
- 708 Seinfeld, J.H., Pandis, S.P., 1998. Atmospheric chemistry and physics: From air pollution to climate  
709 change. Wiley, New York.
- 710 Simpson, D., Fagerli, H., Jonson, J.E., Tsyro, S., Wind, P., Tuovinen, J.P., 2003. Transboundary  
711 acidification and eutrophication and ground level ozone in Europe: Unified EMEP Model  
712 Description, EMEP Status Report 1/2003 Part I, EMEP/MS-CW Report. Oslo.
- 713 Štěpánek, P., Zahradníček, P., Farda, A., 2013. Experiences with data quality control and  
714 homogenization of daily records of various meteorological elements in the Czech Republic in  
715 the period 1961-2010. *Idojaras* 117, 123–141.
- 716 Štěpánek, P., Zahradníček, P., Huth, R., 2011. Interpolation techniques used for data quality control  
717 and calculation of technical series: An example of a Central European daily time series. *Idojaras*

- 718 115, 87–98.
- 719 UNECE, 2004. Handbook for the 1979 convention on long-range transboundary air pollution and its  
720 protocols. New York and Geneva.
- 721 Vestreng, V., Myhre, G., Fagerli, H., Reis, S., Tarrasón, L., 2007. Twenty-five years of continuous  
722 sulphur dioxide emission reduction in Europe. *Atmos. Chem. Phys.* 7, 3663–3681.
- 723 Waldner, P., Marchetto, A., Thimonier, A., Schmitt, M., Rogora, M., Granke, O., Mues, V., Hansen, K.,  
724 Pihl Karlsson, G., Žlindra, D., Clarke, N., Verstraeten, A., Lazdins, A., Schimming, C., Iacoban, C.,  
725 Lindroos, A.-J., Vanguelova, E., Benham, S., Meesenburg, H., Nicolas, M., Kowalska, A., Apuhtin,  
726 V., Napa, U., Lachmanová, Z., Kristoefel, F., Bleeker, A., Ingerslev, M., Vesterdal, L., Molina, J.,  
727 Fischer, U., Seidling, W., Jonard, M., O’Dea, P., Johnson, J., Fischer, R., Lorenz, M., 2014.  
728 Detection of temporal trends in atmospheric deposition of inorganic nitrogen and sulphate to  
729 forests in Europe. *Atmos. Environ.* 95, 363–374. doi:10.1016/j.atmosenv.2014.06.054
- 730



**HIGHLIGHTS**

- Temporal coherence of precipitation  $\text{SO}_4$ ,  $\text{NO}_3$  and  $\text{NH}_4$  was demonstrated
- Regional S and N emissions enabled to reconstruct long-term changes in deposition
- Empirically-based interpolation allowed spatial deposition variations to be mapped

ACCEPTED MANUSCRIPT